studies revealed diffuse demyelinating neuropathy of the motor nerves (supplemental table 1), and needle electromyography showed fibrillation potentials and giant and/or polyphasic motor unit potentials. Motor-evoked potentials demonstrated prolongation in central and peripheral motor conduction times. Somatosensory-evoked potentials showed delayed peripheral sensory conduction (supplemental table 1). Sural nerve biopsy revealed mild loss of myelinated fibres (density =4392.4/mm^2, cf. normal density =6714.2±1560.7/mm^2),[4] and an increase in thinly myelinated fibres (mean axon diameter to fibre diameter ratio =0.76±0.05, cf. normal ratio =0.48±0.06).[4] Lymphocytic infiltration into the endoneurium was also observed (figure 1K–M). Congo red staining revealed no amyloid deposits.

DNA chip resequencing analysis (supplemental methods) of the patient's genomic DNA revealed a heterozygous missense c.6406C>T (p.R2136C) mutation in the *SETX* gene (figure 1P), but no mutation in the remaining 26 Charcot–Marie–Tooth disease-related genes. The patient's parents (figure 1N,O) and sister (figure 1Q) did not carry the mutation. Nor was this mutation detected in 100 chromosomes from healthy individuals or in 850 chromosomes from 425 patients with inherited neuropathy.

The patient was treated with steroid pulse therapy, followed by oral prednisolone therapy (50 mg/day with gradual tapering). He improved clinically, regaining hand (grip strength 2.5 kg/5 kg to 6.5 kg/5.5 kg) and foot function (heel-rise 8 cm/6.5 cm to 9.5 cm/10 cm), as confirmed by quantitative myometry. Dramatic reductions in his shoulder pain and improvements in other sensory and urinary symptoms were also observed over an 8-week period. However, there was no improvement in nerve conduction or spinal MRI, and over a longer period of time, symptoms gradually deteriorated once again.

DISCUSSION

The p.R2136C mutation in *SETX*, which segregated with the disease, was determined to be a de novo mutation in the patient. The p.R2136H mutation, which is located at the same position but involves a different amino acid change, results in typical ALS4.[3] Together with the absence of a *SETX* mutation in controls, these results suggest that p.R2136C is responsible for the ALS4 phenotype in the patient described herein.

The patient exhibited stepwise deterioration with subacute relapses and multifocal asymmetric involvement of peripheral nerves. Although cerebrospinal fluid protein amount was normal, delayed peripheral conduction, enlarged and gadolinium-enhanced nerve roots, thinning of myelin sheaths with lymphocytic infiltrates (which is rarely seen in neurodegenerative diseases), and a response to immunotherapy (as measured by quantitative myometry and compound motor action potential amplitudes) all support the presence of superimposed inflammatory demyelinating neuropathy. Although inflammation may have also occurred in the anterior horns of the spinal cord, this was difficult to evaluate.

Previous reports regarding ALS4 did not detect clinically overt sensory impairment, although the p.L389S mutation results in a slightly elevated vibratory threshold in <10% of affected elderly patients.[1–3 5] Postmortem examinations of patients with the p.L389S mutation revealed neuronal loss in the dorsal root ganglia and degeneration of the posterior columns.[1–3] These results suggest chronic involvement of the sensory nervous system in ALS4. However, inflammatory components, as seen in the present patient, have never been reported. Neuronal degeneration and continuous myelin destruction possibly progressed from childhood. Continuous ongoing nervous tissue destruction and/or disturbed SETX functions in lymphocytes might have led to autoimmune demyelination later in life. Results from the present case report suggest beneficial effects of immune therapy, at least in the short term, when inflammatory radiculoneuropathy coexists in ALS4 patients.

Toru Saiga,[1] Takahisa Tateishi,[1] Takako Torii,[1] Nobutoshi Kawamura,[1] Yuko Nagara,[1] Hiroshi Shigeto,[1] Akihiro Hashiguchi,[2] Hiroshi Takashima,[2] Hiroyuki Honda,[3] Yasumasa Ohyagi,[1] Jun-ichi Kira[1]

[1]Department of Neurology, Neurological Institute, Graduate School of Medical Sciences, Kyushu University, Fukuoka, Japan; [2]Department of Neurology and Geriatrics, Kagoshima University Graduate School of Medical and Dental Sciences, Kagoshima, Japan; [3]Department of Neuropathology, Neurological Institute, Graduate School of Medical Sciences, Kyushu University, Fukuoka, Japan

Correspondence to Professor Jun-ichi Kira, Department of Neurology, Neurological Institute, Graduate School of Medical Sciences, Kyushu University, 3-1-1 Maidashi, Higashi-ku, Fukuoka 812-8582, Japan; kira@neuro.med.kyushu-u.ac.jp

► Additional materials are published online only. To view these files please visit the journal online (http://jnnp.bmj.com/content/83/7.toc).

Contributors TS, T Tateishi, YO and JK carried out clinical studies and wrote the manuscript. HS and T Torii performed electrophysiological examinations. AH and HT carried out genetic studies. YN, NK and HH performed neuropathological studies of the biopsied sural nerve.

Funding This work was supported in part by grants from the Research Committee of Neuroimmunological Diseases, the Ministry of Health, Labour and Welfare, Japan (JK), the Ministry of Education, Culture, Sports, Science and Technology, Japan (JK and HT), and from the Nervous and Mental Disorders and Research Committee for Ataxic Disease of the Ministry of Health, Labour and Welfare, Japan (grant 19A-1, HT).

Competing interests None.

Patient consent Obtained.

Ethics approval Ethics approval was provided by the Institutional Review Board of Kagoshima University.

Provenance and peer review Not commissioned; externally peer reviewed.

Received 17 January 2012
Revised 10 April 2012
Accepted 12 April 2012
Published Online First 10 May 2012

J Neurol Neurosurg Psychiatry 2012;**83**:763–764.
doi:10.1136/jnnp-2012-302281

REFERENCES

1. **Chance PF,** Rabin BA, Ryan SG, *et al.* Linkage of the gene for an autosomal dominant form of juvenile amyotrophic lateral sclerosis to chromosome 9q34. *Am J Hum Genet* 1998;**62**:633–40.
2. **De Jonghe P,** Auer-Grumbach M, Irobi J, *et al.* Autosomal dominant juvenile amyotrophic lateral sclerosis and distal hereditary motor neuronopathy with pyramidal tract signs: synonyms for the same disorder? *Brain* 2002;**125**:1320–5.
3. **Chen YZ,** Bennett CL, Huynh HM, *et al.* DNA/RNA helicase gene mutations in a form of juvenile amyotrophic lateral sclerosis (ALS4). *Am J Hum Genet* 2004;**74**:1128–35.
4. **Chentanez V,** Cha-oumphol P, Kaewsema A, *et al.* Accuracy of the three-window sampling method in morphometric analysis of human sural nerve. *J Neurosci Methods* 2006;**157**:154–7.
5. **Hirano M,** Quinzii CM, Mitsumoto H, *et al.* Senataxin mutations and amyotrophic lateral sclerosis. *Amyotroph Lateral Scler* 2011;**12**:223–7.

Available online at www.sciencedirect.com

SciVerse ScienceDirect

Neuromuscular Disorders 22 (2012) 747–754

www.elsevier.com/locate/nmd

Case study

Inclusion body myositis coexisting with hypertrophic cardiomyopathy: An autopsy study

Yukie Inamori [a], Itsuro Higuchi [a,*], Teruhiko Inoue [b], Yusuke Sakiyama [a], Akihiro Hashiguchi [a], Keiko Higashi [a], Tadafumi Shiraishi [a], Ryuichi Okubo [a], Kimiyoshi Arimura [c], Yoshio Mitsuyama [b], Hiroshi Takashima [a]

[a] *Department of Neurology and Geriatrics, Kagoshima University Graduate School of Medical and Dental Sciences, Kagoshima, Japan*
[b] *Psychogeriatric Center, Daigo Hospital, Miyazaki, Japan*
[c] *Division of Neurology, Okatsu Hospital, Kagoshima, Japan*

Received 24 January 2012; received in revised form 16 March 2012; accepted 28 March 2012

Abstract

Inclusion body myositis is an inflammatory myopathy characterized pathologically by rimmed vacuoles and the accumulation of amyloid-related proteins. Autopsy studies in these patients, including histochemical examinations of multiple skeletal muscles, have not yet been published. In this paper, we describe the autopsy findings of a patient with inclusion body myositis and hypertrophic cardiomyopathy. A 69-year-old man, who was a human T lymphotropic virus type 1 carrier, exhibited slowly progressive muscle weakness and atrophy, predominantly affecting the scapular, quadriceps femoris, and forearm flexor muscles. His disease course was more rapidly progressive than that typically observed; the patient died suddenly of arrhythmia 5 years after diagnosis. Autopsy findings revealed that multiple muscles, including the respiratory muscles, were involved. Longitudinal studies revealed an increased frequency of rimmed vacuoles and p62/sequestosome 1- and/or TAR DNA-binding protein 43-positive deposits in autopsied muscles, although the amount of inflammatory infiltrate appeared to be decreased. We speculated that muscle degeneration may be more closely involved in disease progression compared with autoimmunity. Genetic analysis revealed a myosin binding protein C3 mutation, which is reportedly responsible for familial hypertrophic cardiomyopathy. This mutation and human T lymphotropic virus type 1 infection may have affected the skeletal muscles of this patient.

Keywords: Inclusion body myositis; Hypertrophic cardiomyopathy; Myosin binding protein C3 gene; Autopsy; Human T lymphotropic virus type 1

1. Introduction

Inclusion body myositis (IBM) is an inflammatory myopathy that clinically manifests as slowly progressive proximal and distal muscle weakness and most prominently affects the quadriceps, forearm flexors, and pharyngeal muscles. The etiology of IBM is unknown, and no successful treatment has been reported till date. In addition to inflammatory changes, IBM is pathologically characterized by the presence of rimmed vacuoles and the accumulation of amyloid-related proteins [1–4]. Phenotypic similarities between the muscle fibers of patients with IBM and the brains of patients with Alzheimer's disease have been reported [5–7]. Although IBM is generally sporadic, a few familial cases have been reported [8–13]. The involvement of genetic susceptibility factors in IBM has also been reported [9,14]. To the best of our knowledge, autopsy studies, including histochemical examinations of multiple skeletal muscles and the brain of IBM patients, have not yet been published.

* Corresponding author. Address: Department of Neurology and Geriatrics, Kagoshima University Graduate School of Medical and Dental Sciences, 8-35-1 Sakuragaoka, Kagoshima City, Kagoshima 890-8520, Japan. Tel.: +81 99 275 5332; fax: +81 99 265 7164.
E-mail address: ihiguchi@m2.kufm.kagoshima-u.ac.jp (I. Higuchi).

0960-8966/$ - see front matter © 2012 Elsevier B.V. All rights reserved.
http://dx.doi.org/10.1016/j.nmd.2012.03.011

Hypertrophic cardiomyopathy (HCM) is a myocardial disease characterized by cardiac hypertrophy and diastolic ventricular dysfunction. It often leads to severe heart failure and sudden death. More than 50% patients with HCM have an apparent family history that mainly comprises an autosomal dominant genetic trait; therefore, mutations in the genes for the sarcomere or Z-disc components can be found in patients with familial HCM [15]. A patient with IBM and HCM has been previously reported [16]. This patient was part of a study comprising 40 patients with IBM, 22 of who had additional cardiovascular abnormalities; this patient was among those 22 patients. However, a detailed description of the patient, including histochemical examinations of skeletal and cardiac muscles, was not reported [16].

In this paper, we report the autopsy findings of a patient with IBM associated with HCM. We performed a pathological analysis of multiple muscles and the brain to elucidate the extent of the disease and its longitudinal course. In addition, we analyzed the genetic background of the patient.

2. Patient and methods

2.1. Patient

The patient was a 69-year-old man with a 5-year history of slowly progressive muscle weakness and unsteady walking. His sister had developed progressive muscle weakness and atrophy accompanied by unsteady walking around the age of 60; however, the detailed cause and her background history were unclear. There was no family history of other neuromuscular or cardiovascular diseases. He had a history of mild hypertension and vasospastic angina pectoris; mild left ventricular hypertrophy was detected by echocardiography. Neurological examinations revealed proximal and distal muscle weakness (Medical Research Council grade 2–4/5) as well as atrophy in all four limbs and the neck, scapular, and paraspinal muscles. Regarding laboratory data, the level of serum creatine kinase was 343 IU/l (normal range, 45–163 IU/l). The anti-human T lymphotropic virus type 1 (HTLV-1) antibody was detected in the serum (titer, ×16,384). HTLV-1 proviral load in the peripheral blood mononuclear cells (PBMCs) was 1368 copies per 10^4 PBMCs. Autoimmune analyzes, including tests for anti-Jo-1, anti-nuclear, anti-ribonucleoprotein, anti-Sjogren's syndrome (SS)-A (Ro), and anti-SS-B (La) antibodies, were negative. Thyroid function was normal. Needle electromyography findings indicated mild myopathic features. Short inversion-time inversion recovery magnetic resonance imaging of the buttock muscles revealed severe atrophy of the paraspinal, gluteus maximus, and iliopsoas muscles; in addition, a hyperintense lesion was identified in the gluteus maximus muscle. Muscle biopsy revealed inflammatory myopathy with rimmed vacuoles. The patient was diagnosed with IBM and treated with corticosteroid pulse therapy (methylprednisolone 1 g/day for 3 days), oral prednisolone (40 mg/day), and mizoribine (100 mg/day). Oral prednisolone was tapered, and low-dose prednisolone (5 mg/day) and mizoribine (100 mg/day) were continued; however, his condition worsened, and he became bedridden within a few years. Four years later, the patient developed unstable angina pectoris and underwent percutaneous coronary intervention. Left ventricular hypertrophy without chamber dilation was detected by echocardiography in the absence of any other systemic or cardiac disease that was capable of producing evident wall thickening. Left ventricular outflow tract obstruction was not detected by echocardiography, and he was clinically diagnosed with hypertrophic nonobstructive cardiomyopathy. Five years after being diagnosed with IBM, he developed symptomatic ventricular arrhythmia and died suddenly at his residence. Autopsy was performed 6 h after death, and the findings revealed the presence of cardiomyopathy and the absence of any other cause of death, suggesting that he died of lethal arrhythmia caused by HCM. The patient had provided written informed consent for autopsy studies to be performed after his death, and the study was approved by the institutional review board of Kagoshima University Hospital.

2.2. Histochemical and immunohistochemical studies of the patient's skeletal muscles

For biopsy, skeletal muscle specimens were obtained from the left biceps brachii muscle, and for autopsy, skeletal muscle specimens were obtained from the left biceps brachii, quadriceps femoris, rectus abdominis, diaphragm, and bilateral iliopsoas muscles. Biopsied and autopsied skeletal muscle specimens were immediately frozen in isopentane cooled with liquid nitrogen. Serial frozen sections (thickness, 8 μm) were stained with hematoxylin and eosin (HE) and other histochemical stains, including cytochrome c oxidase (COX). For immunohistochemistry, mouse monoclonal antibodies against CD4 (Dako, Glostrup, Denmark, #M0716; 1:20 dilution), CD8 (Dako, #M0707; 1:20), CD3 (Becton Dickinson, San Jose, CA, USA, #347341; 1:50), CD20 (Dako, #M0755; 1:100), major histocompatibility complex (MHC) class I (Dako, #M0736; 1:500), TAR DNA-binding protein 43 (TDP43) (Protein Tech, Chicago, IL, USA, #60019-2-Ig; 1:100), p62/sequestosome 1 (Santa Cruz, Santa Cruz, CA, USA, #sc-28359; 1:50), myosin binding protein C3 (MYBPC3) (Santa Cruz, #sc-137182; 1:200), titin (Novocastra, Newcastle upon Tyne, UK, 1:100), myosin heavy chain (slow) (Novocastra, 1:50), myosin heavy chain (fast) (Novocastra, 1:20), myosin heavy chain (developmental), (Novocastra, 1:20), and myosin heavy chain (neonatal) (Novocastra, 1:10) were used. Biotinylated anti-mouse immunoglobulin G antibodies were used as secondary antibodies, and the avidin–biotin–peroxidase complex method was used for signal detection (Vecstain Elite ABC kit, Vector Laboratories, Burlingame, CA). All immunohistochemical tests were performed according to previously described methods [17]. The frequency of rimmed or nonrimmed vacuolated fibers and

TDP43-positive deposits in muscle fibers and non-necrotic COX-deficient fibers were determined by photographing a random field and counting 300–500 fibers.

2.3. Histochemical and immunohistochemical studies of the brain

Buffered, formalin-fixed, paraffin-embedded brain sections were stained using HE and Bielschowsky silver staining methods.

2.4. Histochemical studies of the cardiac muscle

Buffered, formalin-fixed, paraffin-embedded cardiac muscle sections were stained with HE.

2.5. Genetic analysis

We screened all coding sequences of the three most prevalent pathogenic HCM genes: cardiac *MYBPC3* (OMIN *600958), β-myosin heavy chain (*MYH7*, OMIN +160760), and cardiac troponin T (*TNNT2*, OMIN *191045) [18,19]. Total DNA was extracted from peripheral blood leukocytes using the DNeasy Blood & Tissue kit (Qiagen, Valencia, CA, USA). We designed primers to amplify exons on the basis of previously reported data [20] and screened the amplified polymerase chain reaction products obtained from the patient's genomic DNA for mutations using an ABI 3010 sequencer (Applied Biosystems, Foster City, CA, USA). We aligned the resulting sequences and evaluated mutations with the Sequencher sequence alignment program (Gene Codes, Ann Arbor, MI, USA).

3. Results

3.1. Histochemical and immunohistochemical studies of skeletal muscles

Biopsy specimens obtained from the left biceps brachii muscle exhibited inflammatory myopathy with rimmed vacuoles. Mononuclear inflammatory cells had accumulated in the endomysium, perimysium, and surrounding vessels. CD8+ cells had invaded the non-necrotic fibers. Diffuse immunoreactivity to MHC class I was observed on the muscle fiber membranes. Connective tissue elements were slightly increased, whereas COX activity was deficient in some fibers. In ATPase-treated sections, hypertrophic type 1 fibers more than 100 μm in diameter were observed (Fig. 1). Vacuolated muscle fibers contained p62- or TDP43-immunoreactive deposits within the vacuoles or the vacuole-free cytoplasm. In addition, there were occasional muscle fibers that did not appear to be vacuolated but contained p62- or TDP43-positive deposits (Fig. 3a–d). These findings fulfilled the criteria of pathologically defined IBM [1].

All autopsied skeletal muscle specimens, including the diaphragm, exhibited inflammatory myopathy with rimmed vacuoles. Each muscle exhibited a different degree of inflammation, and a different frequency of rimmed or nonrimmed vacuolated fibers and p62- and TDP43-positive deposits were observed in each muscle fiber. In addition, each fiber exhibited a different degree of hypertrophy or atrophy. Laterality was obvious in the iliopsoas muscles (Figs. 2a–f, and 3e and f). Compared with biopsied muscles, autopsied muscles exhibited an increased frequency of rimmed vacuoles in the muscle fibers, decreased numbers of inflammatory cells, and no widespread upregulation of MHC class I (Fig. 2g and h). No significant ectopic expression of *MYBPC3* and no defect in titin and myosin heavy chain associated with MYBPC were observed in the skeletal muscles. The histochemical and immunohistochemical findings of multiple muscles are summarized in Table 1.

3.2. Histochemical and immunohistochemical analysis of the brain

The brain weighed 1460 g. Atrophy of the brain, including the hippocampus, was not macroscopically obvious. Senile plaques were rare, and no extensive neuronal loss was microscopically observable. Neurofibrillary tangles were mildly present in the hippocampus and parahippocampal gyrus but rare in the neocortex on the lateral surface of the temporal lobe. These neurofibrillary tangle pathologies, which occur commonly with aging, corresponded to Braak stage II. No obvious change associated with Alzheimer's disease was observed in the brain.

3.3. Pathological studies of the cardiac muscle

Left ventricular hypertrophy without chamber dilation was macroscopically observed, whereas hypertrophy (27.2 ± 7.8 mm in diameter), disarray, and expanded fibrosis of the myocytes were microscopically observed. Inflammatory cells were not observed. Some myocytes had degenerative vacuoles, but it could not be determined whether they were rimmed because the cardiac muscles were embedded in paraffin (Fig. 4).

3.4. Genetic analysis

By direct sequencing, we screened each coding exon of *MYBPC3*, *MYH7*, and *TNNT2* for mutations. Among them, a heterozygous p.T1046M (c. C3137T) missense mutation in *MYBPC3* was identified. This mutation was previously reported as one of the mutations responsible for HCM [21].

4. Discussion

We described the autopsy findings of a patient who presented with HCM during the course of biopsy-proven IBM. The patient met the clinical and pathological criteria for HCM [15] and IBM [1]. As cardiomyopathy is very rarely described in association with sporadic IBM, we

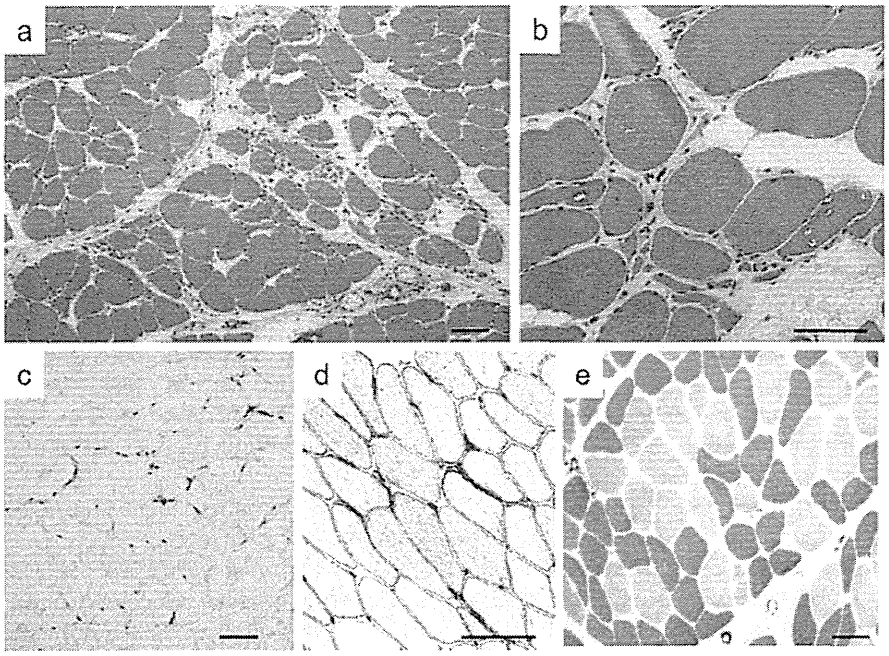

Fig. 1. Histochemical and immunohistochemical staining of biopsied skeletal muscles of the patient. Hematoxylin and eosin staining revealed inflammatory myopathy with rimmed vacuoles (a, b). Immunohistochemistry for CD8 reveals the infiltration of CD8+ T-lymphocytes (c). Upregulation of sarcolemmal major histocompatibility complex class I expression (d). ATPase staining (pH 10.4) reveals some hypertrophic type 1 muscle fibers, which were more than 100 μm in diameter, and many atrophic fibers of various muscle types (e). Bar scale, 100 μm.

searched for other causes of HCM and found a mutation in *MYBPC3*.

The *MYBPC3* mutation identified in this patient is reportedly responsible for familial HCM [21]. The patient's elder sister had suffered a similar, unspecified disease characterized by progressive muscle atrophy. Although the patient exhibited prominent dysfunction of the quadriceps femoris and forearm flexor muscles, which is characteristic of IBM, he also displayed marked atrophy and weakness of the scapular muscles at an earlier stage compared with other sporadic IBM patients. Furthermore, he became bedridden within a few years of IBM diagnosis and exhibited a more rapidly progressive course than that typically observed for IBM.

To the best of our knowledge, a histochemical study of multiple muscles affected by IBM has not yet been published. In our study, all examined muscles exhibited pathological changes associated with the disease; however, the degree of inflammation, mitochondrial abnormalities, atrophy, or hypertrophy and the frequency of rimmed vacuoles and TDP43- or p62-positive deposits in the muscle fibers were muscle-specific. The laterality of pathological findings was obvious, which reflected the clinical presentation of asymmetric muscle atrophy. Despite the lack of clinical respiratory impairment, the diaphragm muscles were involved. The quadriceps femoris muscle, which was affected at an early stage of the disease, contained rare hypertrophic fibers, as did the right iliopsoas muscle, which was clinically affected more severely than the left iliopsoas muscle. On the contrary, the left biceps brachii and left iliopsoas muscles, which comparatively maintained muscle strength, contained many hypertrophic fibers. These findings suggest that clinical muscle strength may correlate with the number of hypertrophic fibers. COX-deficient muscle fibers and large-scale mitochondrial DNA deletions are more frequent in patients with sporadic IBM than in age-matched controls, although COX-deficient muscle fibers increase with age [22]. In patients with sporadic IBM and a high number of COX-deficient fibers, impaired mitochondrial function probably contributes to muscle weakness and wasting [23]. In this patient, the frequency of non-necrotic, COX-deficient fibers in the left quadriceps femoris muscle, which was affected at an early stage of the disease, was higher than that in other muscles. Furthermore, the frequency of non-necrotic, COX-deficient fibers in the right iliopsoas muscle was higher than that in the left iliopsoas muscle, and the former was clinically affected more severely than the latter. Mitochondrial abnormalities may also have affected clinical muscle strength in this patient.

Longitudinal histochemical and immunohistochemical analyzes suggested that muscle degeneration due to the ubiquitin–proteasome system and autophagosomal–lysosomal pathway dysfunction may be more closely involved in IBM progression compared with autoimmunity. The frequency of rimmed vacuoles had increased in the autopsied muscles, although the amount of inflammatory infiltrate had decreased because of immunotherapy or the natural course of the disease. In addition, we revealed that the frequency of p62- or TDP43-positive deposits in the fibers of the left biceps brachii increased over time. p62, also known

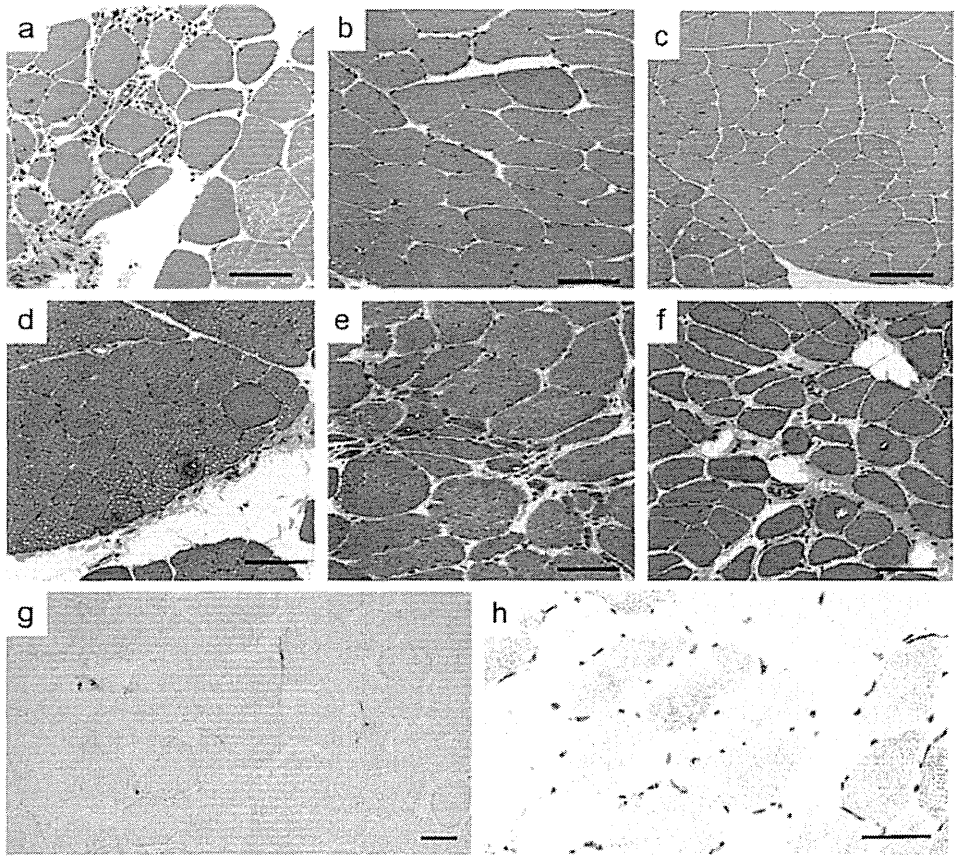

Fig. 2. Histochemical and immunohistochemical staining of autopsied skeletal muscles of the patient (a) left biceps brachii, (b) left quadriceps femoris, (c) left rectus abdominis, (d) right iliopsoas, (e) left iliopsoas, (f) diaphragm. Hematoxylin and eosin staining reveals the different degrees of inflammatory infiltration, fiber atrophy, and fiber hypertrophy. The muscle fiber size is different in each muscle. Immunohistochemical staining for CD8 and major histocompatibility complex (MHC) class I revealed that CD8+ cells are rare in autopsied muscles (g). The widespread upregulation of MHC class I was not observed in autopsied muscles (h). Bar scale, 100 μm.

as sequestosome 1, is a shuttle protein that transports polyubiquitinated proteins for both proteasomal and lysosomal degradation [24]. The expression of p62 is increased at both the protein and mRNA levels, and it is strongly accumulated within and as a dense peripheral shell surrounding p-tau-containing inclusions in IBM muscle fibers [25]. TDP43 was recently identified in normal muscle nuclei and the sarcoplasm as well as around some rimmed vacuoles in patients with IBM. The significance of TDP43 accumulation is currently unclear, but it may be related to ubiquitin–proteasome system dysfunction [26]. The progression of mitochondrial abnormalities was not confirmed in this study. We speculate that degenerative processes, rather than inflammatory processes, mainly contribute to muscle fiber destruction and progressive muscle wasting in the advanced stages of IBM. However, an interrelationship between inflammation and degeneration is considered important in the early stages of IBM, and the early initiation of anti-inflammatory therapy may be useful in treating this disease.

Inflammatory changes have also been reported in other degenerative diseases. A few individual patients with Charcot–Marie–Tooth type 1 (CMT1) disease have reportedly responded to anti-inflammatory treatment [27]. Unlike most patients with CMT1, these patients exhibited inflammatory infiltration in nerve biopsy specimens. In addition, the administration of rituximab increased muscle strength in two patients with dysferlin-deficient muscular dystrophy, and these patients exhibited inflammatory infiltration in muscle biopsy specimens [28]. These findings suggest a relationship between genetic defects and immune system abnormalities. Therefore, the association between degeneration and inflammation is a complex and multifactorial issue.

Aspects of IBM pathology share intriguing similarities with those of Alzheimer's disease, the most common form of elderly dementia [5–7]. A patient with clinically diagnosed Alzheimer's disease and biopsy-proven IBM has been reported [29]. Histochemical investigations of the brains of patients with IBM have not yet been published, nor have any epidemiological links between IBM and Alzheimer's disease. Nevertheless, the patient did not exhibit any clinical features of dementia or pathological changes associated with Alzheimer's disease.

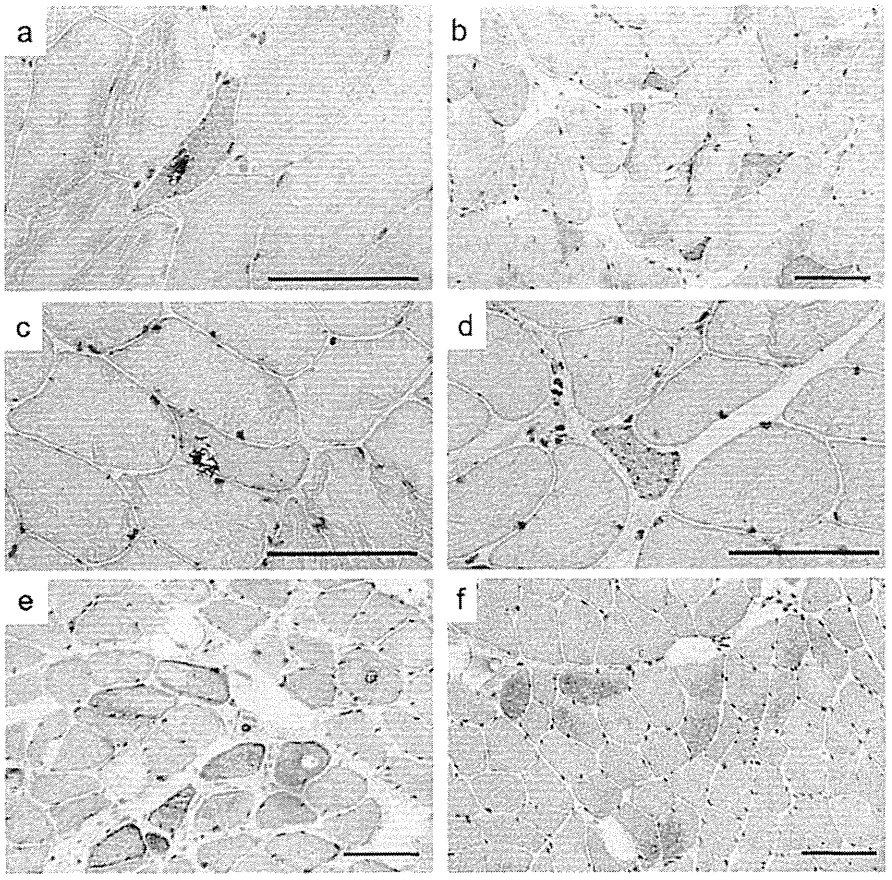

Fig. 3. Immunohistochemical staining of biopsied and autopsied skeletal muscles of the patient. p62-positive deposits (a, b) and TDP43-positive deposits (c, d) are observed within the vacuoles or the vacuole-free cytoplasm in the biopsied skeletal muscles. Compared with that in biopsied skeletal muscles, the frequency of p62- (e) or TDP43-positive (f) deposits is higher in autopsied skeletal muscles. Bar scale, 100 μm.

Table 1
Comparison of the histochemical and immunohistochemical findings between multiple muscles.

		RV (%)	COX (−) (%)	Inflammatory cells	Atrophic fibers	Hypertrophic fibers	P62 (+) (%)	TDP43 (+) (%)
Biopsied muscles	lt BB	0.73	1.5	+++	++	+	4.7	0.3
Autopsied muscles	lt BB	1.36	1	±	+++	+++	12.5	2
	lt QF	0.25	2.6	±	+	±	2.0	1.7
	lt RA	1.2	1.6	±	+	±	0.8	4.2
	lt IP	3.9	0.31	+	+++	+++	14.9	1.3
	rt IP	2.6	1.75	+	+	±	4.4	2.4
	lt diaphragm	2.2	0.24	+	+	±	6.3	2.8

The frequency of rimmed or nonrimmed vacuolated fibers and TDP43-positive deposits in muscle fibers and non-necrotic COX-deficient fibers is shown. The frequency of inflammatory cells, atrophic fibers, and hypertrophic fibers is shown from ± (rare) to +++ (many).
BB, biceps brachii muscle; QF, quadriceps femoris muscle; RA, rectus abdominis muscles; IP, iliopsoas muscles; RV, rimmed or nonrimmed vacuolated fibers; COX (−), non-necrotic COX-deficient fibers; p62 (+), fibers that contained p62-positive deposits; TDP43 (+), fibers that contained TDP43-positive deposits.

MYBPC is essential for the structure of the sarcomere in striated muscles. Two types of MYBPC are expressed in skeletal muscle (MYBPC1 and MYBPC2), whereas one type is expressed in cardiac muscle (cardiac MYBPC; *MYBPC3*). Mutations in *MYBPC3* account for approximately 15% cases of familial HCM. By binding to myosin heavy chain and the cytoskeletal protein titin, cardiac MYBPC contributes to the structural integrity of the sarcomere, and it may also regulate cardiac contractility in response to adrenergic stimulation. The T1046M mutation in *MYBPC3* is located in the C8 region, which has a binding site for titin [30]. The onset of clinical symptoms following *MYBPC3* mutations is often delayed until middle or old age. Delayed expression of cardiac hypertrophy and a

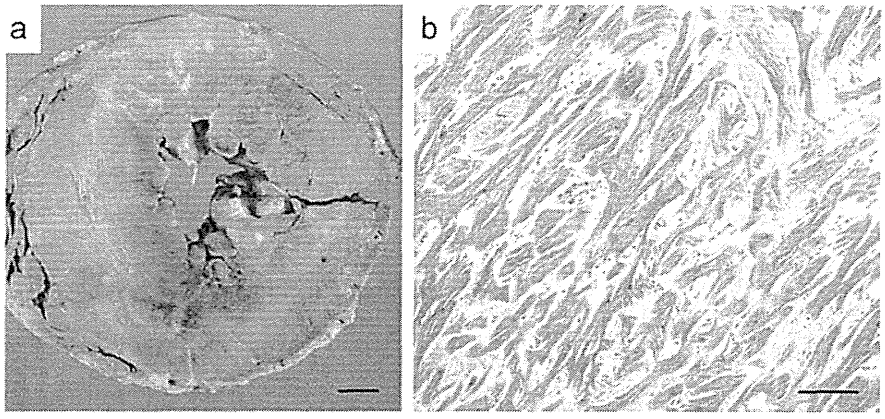

Fig. 4. Autopsy cardiac muscles of the patient (a, b). Left ventricular hypertrophy without chamber dilation is macroscopically observed (a). Hypertrophy, disarray, and expanded fibrosis of the myocytes are microscopically observed in the patient. Inflammatory cells are not observed, whereas some myocytes with vacuoles are observed (b). Bar scale, (a) 10 mm and (b) 100 μm.

favorable clinical course were reported to be markedly different from the clinical course related to mutations caused by other genetic causes in patients with HCM [31]. Cardiac MYBPC is not expressed in normal skeletal muscle, not even during development [32]. Interestingly, a female infant with fatal cardiomyopathy due to a homozygous mutation, p.R943X, in *MYBPC3* and unexpected skeletal myopathy has been reported [33]. The patient expressed the cardiac-specific MYBPC isoform in skeletal muscle at the transcript and protein levels. Numerous muscle fibers expressing the mutant cardiac isoform displayed structural abnormalities with sarcomere disorganization and myosin thick filament depletion, although the reason for the ectopic expression of cardiac MYBPC remains unknown [33]. Ectopic expression of *MYBPC3* or obvious abnormal immunoreactivity of titin was not detected in the skeletal muscle of our patient. Because he exhibited some atypical aspects of IBM, the *MYBPC3* T1046M mutation may have affected the clinical severities or pathological findings, similar to type 1 muscle fiber hypertrophy.

Although IBM is generally sporadic, a few familial cases have been reported [8–13]. The involvement of genetic susceptibility factors in IBM has also been reported [9,14]. The patient's sister had an unspecified progressive muscle atrophic disease, suggesting that skeletal muscle disease may occur on a familial basis. In addition, the patient exhibited anti-HTLV-1 antibody positivity in the serum and a high HTLV-1 viral load in the PBMCs. HTLV-1 infection is reported to be one of the possible causes of sporadic IBM. Eleven IBM patients with serum anti-HTLV-1 antibodies have been reported from an endemic area in Japan, and the clinical or pathological findings of nine of these patients were no different from those in other sporadic IBM patients. The remaining two patients exhibited familial occurrence [34]. A 58-year-old woman with IBM and HTLV-1 infection exhibited no difference in apparent clinical or pathological findings compared with other sporadic IBM patients, excluding higher levels of muscle enzymes [35]. A 49-year-old woman with IBM and HTLV-1 infection exhibited considerable wasting and weakness of the shoulder girdle and quadriceps muscle in addition to respiratory muscle weakness, which caused hypercapnic respiratory failure requiring mechanical ventilator support [36]. Therefore, some unusual aspects have been reported in rare cases of IBM associated with HTLV-1 infection. HTLV-1 infection may have also affected the development of IBM in this patient. Conversely, there has been no report of an association between HTLV-1 infection and cardiac disorders. Infiltration of atypical lymphocytes was not observed in the skeletal and cardiac muscles of our patient. Although the development of HCM in this patient may have been coincidental, the *MYBPC3* T1046M mutation may have been involved in the pathogenesis of IBM along with HTLV-1 infection.

In summary, we described the autopsy findings of a patient with IBM and HCM. A mutation in *MYBPC3* was identified as the cause of HCM in this patient. Multiple muscles, including the respiratory muscles, were involved, although no brain involvement was observed. Longitudinal studies revealed that muscle degeneration due to ubiquitin–proteasome system and autophagosomal–lysosomal pathway dysfunction may be more closely involved in the progression of IBM compared with autoimmunity. Furthermore, it may be possible that the *MYBPC3* mutation also affected skeletal muscles along with HTLV-1 infection. We suggest that the mutation may be one of the genetic modifiers of IBM, although further clinical and pathological studies are necessary to verify this issue. IBM is believed to be heterogeneous, and its exact etiology has not yet been identified. We believe that this study provides clues that identify the potential underlying causes of IBM and could be valuable in elucidating the extent of the clinical spectrum of this disease.

Acknowledgments

We thank Ms. N. Hirata, Ms. Y. Shirahama, and Ms. A. Yoshimura of our department for their excellent technical

assistance. This work was supported by grants-in-aid for research on intractable diseases and Applying Health Technology from the Ministry of Health, Labour and Welfare, Japan.

References

[1] Benveniste O, Hilton-Jones D. International workshop on inclusion body myositis held at the institute of myology, Paris, on 29 May 2009. Neuromuscul Disord 2010;20:414–21.
[2] Bohan A, Peter JB. Polymyositis and dermatomyositis (second of two parts). N Engl J Med 1975;292:403–7.
[3] Bohan A, Peter JB. Polymyositis and dermatomyositis (first of two parts). N Engl J Med 1975;292:344–7.
[4] Engel WK, Askanas V. Inclusion-body myositis: clinical, diagnostic, and pathologic aspects. Neurology 2006;66:20–9.
[5] Finch CE. A perspective on sporadic inclusion-body myositis: the role of aging and inflammatory processes. Neurology 2006;66:1–6.
[6] Murphy MP, Golde TE. Inclusion-body myositis and Alzheimer disease: two sides of the same coin, or different currencies altogether? Neurology 2006;66:65–8.
[7] Askanas V, Engel WK. Inclusion-body myositis: a myodegenerative conformational disorder associated with Abeta, protein misfolding, and proteasome inhibition. Neurology 2006;66:39–48.
[8] Amato AA, Shebert RT. Inclusion body myositis in twins. Neurology 1998;51:598–600.
[9] Garlepp MJ, Laing B, Zilko PJ, Ollier W, Mastaglia FL. HLA associations with inclusion body myositis. Clin Exp Immunol 1994;98:40–5.
[10] Hengstman GJ, van Engelen BG, ter Laak HJ, Gabreels-Festen AA. Familial inclusion body myositis with histologically confirmed sensorimotor axonal neuropathy. J Neurol 2000;247:882–4.
[11] Mastaglia F, Price P, Walters S, Fabian V, Miller J, Zilko P. Familial inclusion body myositis in a mother and son with different ancestral MHC haplotypes. Neuromuscul Disord 2006;16:754–8.
[12] Sivakumar K, Semino-Mora C, Dalakas MC. An inflammatory, familial, inclusion body myositis with autoimmune features and a phenotype identical to sporadic inclusion body myositis. Studies in three families. Brain 1997;120:653–61.
[13] Tateyama M, Saito N, Fujihara K, et al. Familial inclusion body myositis: a report on two Japanese sisters. Intern Med 2003;42:1035–8.
[14] Argov Z, Eisenberg I, Mitrani-Rosenbaum S. Genetics of inclusion body myopathies. Curr Opin Rheumatol 1998;10:543–7.
[15] Seidman JG, Seidman C. The genetic basis for cardiomyopathy: from mutation identification to mechanistic paradigms. Cell 2001;104:557–67.
[16] Lotz BP, Engel AG, Nishino H, Stevens JC, Litchy WJ. Inclusion body myositis. Observations in 40 patients. Brain 1989;112:727–47.
[17] Higuchi I, Niiyama T, Uchida Y, et al. Multiple episodes of thrombosis in a patient with Becker muscular dystrophy with marked expression of utrophin on the muscle cell membrane. Acta Neuropathol 1999;98:313–6.
[18] Konno T, Chang S, Seidman JG, Seidman CE. Genetics of hypertrophic cardiomyopathy. Curr Opin Cardiol 2010;25:205–9.
[19] Maron BJ. The 2009 international hypertrophic cardiomyopathy summit. Am J Cardiol 2010;105:1164–8.
[20] Millat G, Chanavat V, Crehalet H, Rousson R. Development of a high resolution melting method for the detection of genetic variations in hypertrophic cardiomyopathy. Clin Chim Acta 2010;411:1983–91.
[21] Bahrudin U, Morisaki H, Morisaki T, et al. Ubiquitin–proteasome system impairment caused by a missense cardiac myosin-binding protein C mutation and associated with cardiac dysfunction in hypertrophic cardiomyopathy. J Mol Biol 2008;384:896–907.
[22] Oldfors A, Larsson NG, Lindberg C, Holme E. Mitochondrial DNA deletions in inclusion body myositis. Brain 1993;116:325–36.
[23] Oldfors A, Moslemi AR, Jonasson L, Ohlsson M, Kollberg G, Lindberg C. Mitochondrial abnormalities in inclusion-body myositis. Neurology 2006;66:49–55.
[24] Bjorkoy G, Lamark T, Johansen T. P62/SQSTM1: a missing link between protein aggregates and the autophagy machinery. Autophagy 2006;2:138–9.
[25] Nogalska A, Terracciano C, D'Agostino C, King Engel W, Askanas V. p62/SQSTM1 is overexpressed and prominently accumulated in inclusions of sporadic inclusion-body myositis muscle fibers, and can help differentiating it from polymyositis and dermatomyositis. Acta Neuropathol 2009;118:407–13.
[26] Weihl CC, Temiz P, Miller SE, et al. TDP-43 accumulation in inclusion body myopathy muscle suggests a common pathogenic mechanism with frontotemporal dementia. J Neurol Neurosurg Psychiatry 2008;79:1186–9.
[27] Ginsberg L, Malik O, Kenton AR, et al. Coexistent hereditary and inflammatory neuropathy. Brain 2004;127:193–202.
[28] Lerario A, Cogiamanian F, Marchesi C, et al. Effects of rituximab in two patients with dysferlin-deficient muscular dystrophy. BMC Musculoskelet Disord 2010;11:157.
[29] Roos PM, Vesterberg O, Nordberg M. Inclusion body myositis in Alzheimer's disease. Acta Neurol Scand 2011;124:215–7.
[30] Kulikovskaya I, McClellan G, Flavigny J, Carrier L, Winegrad S. Effect of MyBP-C binding to actin on contractility in heart muscle. J Gen Physiol 2003;122:761–74.
[31] Niimura H, Bachinski LL, Sangwatanaroj S, et al. Mutations in the gene for cardiac myosin-binding protein C and late-onset familial hypertrophic cardiomyopathy. N Engl J Med 1998;338:1248–57.
[32] Gautel M, Furst DO, Cocco A, Schiaffino S. Isoform transitions of the myosin binding protein C family in developing human and mouse muscles: lack of isoform transcomplementation in cardiac muscle. Circ Res 1998;82:124–9.
[33] Tajsharghi H, Leren TP, Abdul-Hussein S, et al. Unexpected myopathy associated with a mutation in *MYBPC3* and misplacement of the cardiac myosin binding protein C. J Med Genet 2010;47:575–7.
[34] Matsuura E, Umehara F, Nose H, et al. Inclusion body myositis associated with human T-lymphotropic virus-type I infection: eleven patients from an endemic area in Japan. J Neuropathol Exp Neurol 2008;67:41–9.
[35] Cupler EJ, Leon-Monzon M, Miller J, Semino-Mora C, Anderson TL, Dalakas MC. Inclusion body myositis in HIV-1 and HTLV-1 infected patients. Brain 1996;119:1887–93.
[36] Littleton ET, Man WD, Holton JL, et al. Human T cell leukaemia virus type I associated neuromuscular disease causing respiratory failure. J Neurol Neurosurg Psychiatry 2002;72:650–2.

Alanyl-tRNA synthetase mutation in a family with dominant distal hereditary motor neuropathy

Z. Zhao, MS
A. Hashiguchi, MD
J. Hu, MD, PhD
Y. Sakiyama, MD, PhD
Y. Okamoto, MD, PhD
S. Tokunaga, MD
L. Zhu, MB
H. Shen, MS
H. Takashima, MD, PhD

Correspondence & reprint requests to Dr. Hu: jinghujp@yahoo.com.cn

ABSTRACT

Objective: To identify a new genetic cause of distal hereditary motor neuropathy (dHMN), which is also known as a variant of Charcot-Marie-Tooth disease (CMT), in a Chinese family.

Methods: We investigated a Chinese family with dHMN clinically, electrophysiologically, and genetically. We screened for the mutations of 28 CMT or related pathogenic genes using an originally designed microarray resequencing DNA chip.

Results: Investigation of the family history revealed an autosomal dominant transmission pattern. The clinical features of the family included mild weakness and wasting of the distal muscles of the lower limb and foot deformity, without clinical sensory involvement. Electrophysiologic studies revealed motor neuropathy. MRI of the lower limbs showed accentuated fatty infiltration of the gastrocnemius and vastus lateralis muscles. All 4 affected family members had a heterozygous missense mutation c.2677G>A (p.D893N) of alanyl-tRNA synthetase (*AARS*), which was not found in the 4 unaffected members and control subjects.

Conclusion: An *AARS* mutation caused dHMN in a Chinese family. *AARS* mutations result in not only a CMT phenotype but also a dHMN phenotype. ***Neurology*® 2012;78:1644-1649**

GLOSSARY

AARS = alanyl-tRNA synthetase; **CMT** = Charcot-Marie-Tooth; **dHMN** = distal hereditary motor neuropathy; **MRC** = Medical Research Council; **SCV** = sensory nerve conduction velocity.

Distal hereditary motor neuropathy (dHMN) is also known as distal spinal muscular atrophy or a variant of Charcot-Marie-Tooth disease (CMT). dHMN is genetically and clinically heterogeneous. It has been classified into 7 subtypes according to age at onset, mode of inheritance, and the presence of additional features.[1] To date, at least 11 genes have been shown to be involved in dHMN: heat shock 27 kDa protein 1 (*HSPB1*), heat shock 22 kDa protein 8 (*HSPB8*), heat shock 27 kDa protein 3 (*HSPB3*), dynactin 1 (*DCTN1*), glycyl-tRNA synthetase (*GARS*), pleckstrin homology domain containing, family G (with RhoGef domain) member 5 (*PLEKHG5*), Berardinelli-Seip congenital lipodystrophy 2 (*BCSL2*), senataxin (*SETX*), immunoglobulin mu binding protein 2 (*IGHMBP2*), ATPase and Cu^{2+} transporting, alpha polypeptide (*ATP7A*), and transient receptor potential cation channel, subfamily V, member 4 (*TRPV4*).[2] Interestingly, 5 of these genes (*HSPB8*, *HSPB1*, *GARS*, *TRPV4*, and *BCSL2*) have been described in CMT[2-6]; in some patients, dHMN and CMT phenotypes have been found to coexist.[7]

Four aminoacyl-tRNA synthetases (AARSs) have been implicated in CMT/dHMN:) glycyl (*GARS*; MIM 601472) in CMT2D and dHMN5A; 2) tyrosyl (*YARS*; MIM 608323) in dominant intermediate CMT type C; 3) alanyl (*AARS*; MIM 613287) in CMT2N; and 4) lysyl (*KARS*; MIM 601421) in CMT-recessive intermediate B and hereditary neuropathy with

From the Departments of Neuromuscular Disease (Z.Z., J.H., H.S.) and Electromyography (L.Z.), Third Hospital of Hebei Medical University, Shijiazhuang, PR China; and Department of Neurology and Geriatrics (A.H., Y.S., Y.O., S.T., H.T.), Kagoshima University Graduate School of Medical and Dental Sciences, Kagoshima, Japan.

Study funding: Supported in part by grants from the Nervous and Mental Disorders and Research Committee for Charcot-Marie-Tooth Disease, Neuropathy, Ataxic Disease and Practical Realization Research for Incurable Disease of the Japanese Ministry of Health, Welfare and Labor (H.T.).

Go to Neurology.org for full disclosures. Disclosures deemed relevant by the authors, if any, are provided at the end of this article.

liability to pressure palsies.[5,8–10] Although mutations in *AARS* cause axonal CMT, no published reports linking *AARS* mutations to the dHMN phenotype exist.

We report clinical and electrophysiologic findings in 3 patients with dHMN from a Chinese family carrying a novel missense mutation (D893N) in AARS.

METHODS

We studied 3 generations of a Chinese family that included 4 affected and 8 unaffected members ascertained by neurologic examination (figure 1).

Patients. ***Patient 1.*** Patient 1 (III-1), now a 16-year-old boy, was referred to our neuromuscular disease department at the age of 11 years. He reported frequent falling and difficulty in rising from the squatting position since the age of 2 years; however, his condition had not deteriorated. Neurologic examination was initially performed at the first referral. His gait was almost normal, with no ataxia, but standing on his heels was difficult, and his heels could not touch the ground when squatting. Mild atrophy and weakness in the distal muscles of the lower limbs were observed, with a muscle strength score of 4 of 5 (Medical Research Council [MRC] scale) for the extensor digitorum brevis muscles, whereas the muscle strength scores of the iliopsoas, quadriceps femoris, biceps femoris, anterior tibial, and gastrocnemius muscles were 5 of 5 (MRC scale). However, the muscle strength of the quadriceps femoris and gastrocnemius muscles was relatively weaker than that of the iliopsoas or anterior tibial muscles. Pes cavus and toe clawing were noted (figure 2A). Sensory examination, including pain sensation, light touch sensation, position sensation, and vibration sensation of the 4 limbs was unremarkable. Deep tendon reflexes were decreased in the knees and absent in the ankles. Examination of the upper limbs was normal. There was no evidence of tremor or pyramidal tract signs.

Patient 2. Patient 2 (I-2), the 67-year-old grandmother of the proband, first showed mild motor disability of the lower limbs at 55 years of age. Physical examination revealed distal motor weakness, wasting in the lower limbs, and pes cavus (figure 2B). Results of sensory examination including pain sensation, light touch sensation, position sensation, and vibration sensation of the 4 limbs were unremarkable. Deep tendon reflexes were absent in the lower limbs. Examination of the upper limbs was normal. There was no evidence of ataxia, tremor, or pyramidal tract signs.

Patient 3 and patient 4. Neither patient 3 (II-1), the 44-year-old father, nor patient 4 (II-3), the 38-year-old aunt, of the proband experienced symptoms; however, neurologic examination revealed foot deformity, mild atrophy, and weakness of the lower limbs. The results of the sensory examination of patients 3 and 4 were similar to those of patients 1 and 2. Deep tendon reflexes were decreased in the knees and absent in the ankles.

Standard protocol approvals, registrations, and patient consent. The patients and family members included in this study gave written informed consent, and the study was approved by the Third Hospital of Hebei Medical University and the Institutional Review Board of Kagoshima University.

Electrophysiologic study. Needle EMG and nerve conduction velocity studies were performed in patients 1, 2, and 3.

MRI study. Skeletal muscle MRI of the lower limbs was performed in patient 1.

Mutation screening. Genomic DNA of 8 family members (I-1, I-2, II-1, II-2, II-3, II-5, III-1, and III-2) was extracted from the peripheral blood obtained using standard methods. The purpose-built GeneChip CustomSeq Resequencing Array (Affymetrix, Inc., Santa Clara, CA) was designed to screen for CMT and related diseases such as ataxia with oculomotor apraxia types 1 and 2, spinocerebellar ataxia with axonal neuropathy, and dHMN. We designed 363 primer sets to cover the entire coding regions and flanking sequences of the following 28 pathogenic genes: early growth response 2 (*EGR2*), peripheral myelin protein 22 (*PMP22*), myelin protein zero (*MPZ*), gap junction protein beta 1 (*GJB1*), periaxin (*PRX*), lipopolysaccharide-induced TNFα factor (*LITAF*), neurofilament light chain polypeptide (*NEFL*), ganglioside-induced differentiation-associated protein 1 (*GDAP1*), myotubularin-related protein 2 (*MTMR2*), SH3 domain and tetratricopeptide repeats 2 (*SH3TC2*), SET-binding factor 2 (*SBF2*), N-myc downstream regulated 1 (*NDRG1*), mitofusin 2 (*MFN2*), Ras-related GTPase 7 (*RAB7*), *GARS*, *HSPB1*, *HSPB8*, lamin A/C (*LMNA*), dynamin 2 (*DNM2*), *YARS*, *AARS*, *KARS*, aprataxin (*APTX*), senataxin (*SETX*), tyrosyl-DNA phosphodiesterase 1 (*TDP1*), desert hedgehog (*DHH*), gigaxonin 1 (*GAN1*), and K-Cl cotransporter 3 (*KCC3*) and 9 other candidate genes. The 363 PCR amplicons were amplified in 32 multiplex PCR reactions using the Qiagen Multiplex PCR system (Qiagen, Venlo, The Netherlands). Each reaction required 120 ng of genomic DNA, 10 pmol of primer sets, dNTP, and Qiagen Multiplex PCR Master Mix (Qiagen). The following conditions were used for multiplex PCR: 15 minutes at 95°C; 42 cycles of amplification (94°C for 30 s, 60°C for 3 minutes, and 72°C for 90 s); and 15 minutes at 68°C. Pooling, DNA fragmentation, labeling, and chip hybridization were performed according to the CustomSeq Resequencing protocol (Affymetrix, Inc.). Chips were washed using a Fluidics Station 450 (Affymetrix, Inc.) using CustomSeq Resequencing wash protocols. Analysis of microarray data was performed using GeneChip Sequence Analysis Software, version 4.0 (Affymetrix, Inc.).[11]

To confirm the mutation revealed by our DNA chip, the proband and 7 members of the family underwent genetic analy-

Figure 1 **Pedigree of the distal hereditary motor neuropathy family**

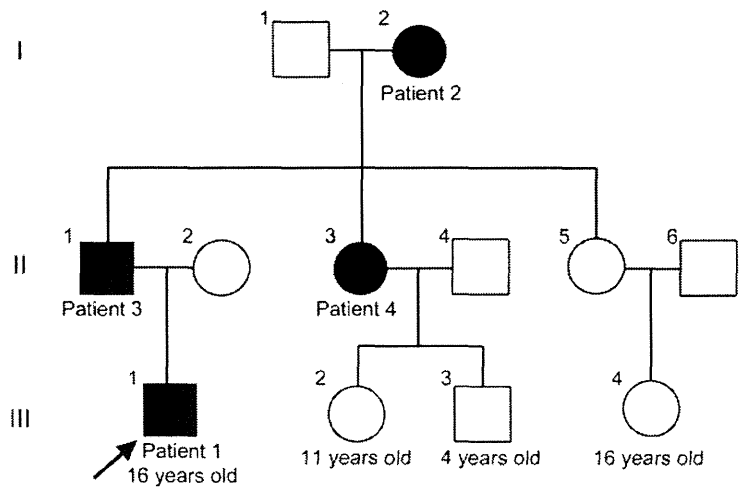

The arrow indicates the proband. Affected individuals are represented by solid black symbols; open symbols represent healthy individuals.

Figure 2 **Clinical, radiologic, and genetic findings of the distal hereditary motor neuropathy family**

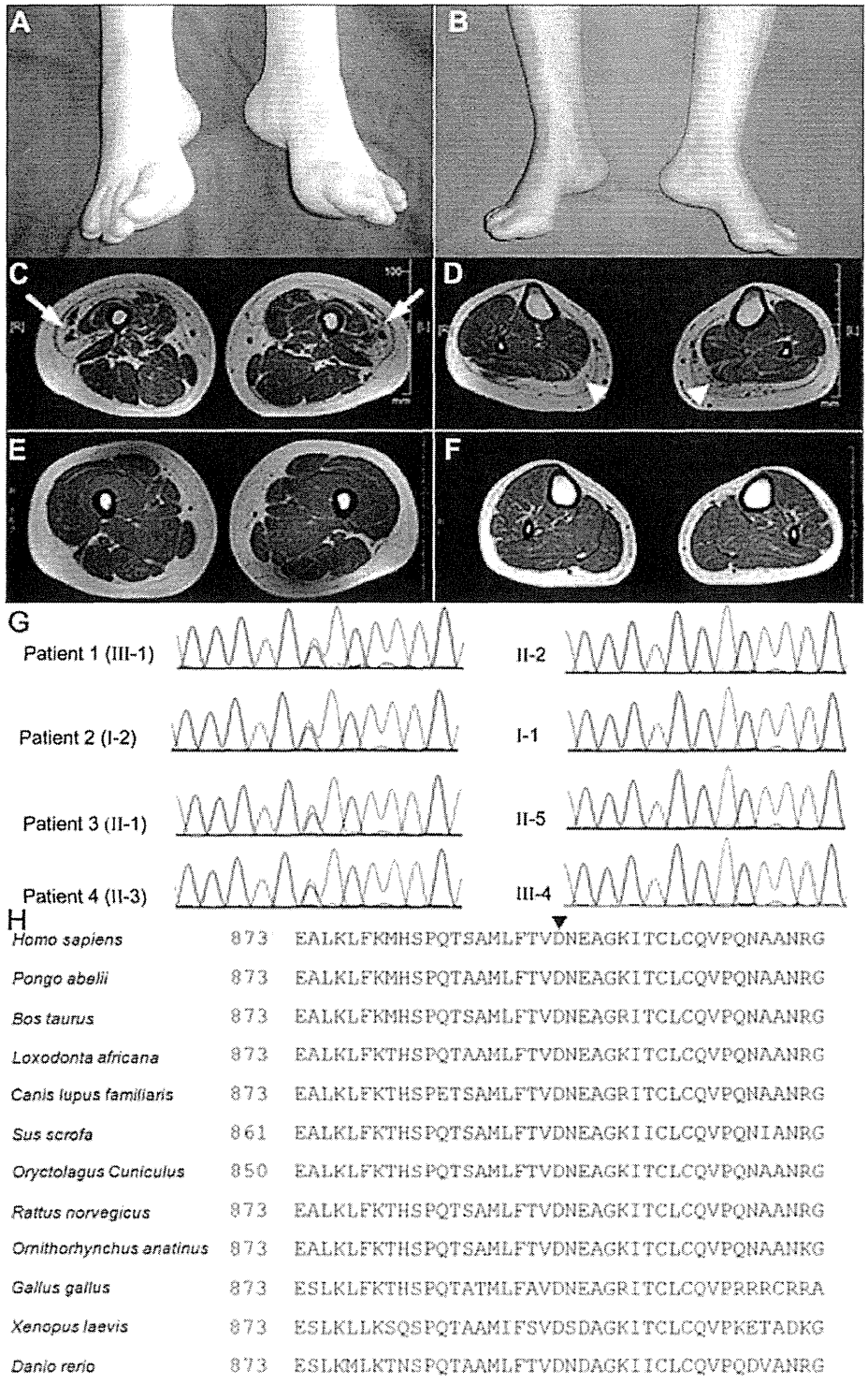

(A) A picture of patient 1 shows moderate pes cavus and toe clawing. (B) A picture of patient 2 shows pes cavus. (C and D) Axial T1-weighted images of the lower limbs in patient 1. (C) Axial image of the thighs, illustrating marked fatty replacement of the vastus lateralis muscle (arrows). (D) Axial image of the legs demonstrating complete fatty replacement of the gastrocnemius muscle (arrowheads). (E and F) Axial T1-weighted images of the lower limbs of a healthy control subject. (G) Chromatogram of the heterozygous c.2677G>A (p.D893N) mutation in exon 19 of *AARS*: left, 4 affected members; right, 4 unaffected relatives. (H) Comparison of AARS from different species. Arrowhead (▼) on top of the alignment indicates 893 amino acids.

Table **Nerve conduction studies in patients 1, 2, and 3**

	Patient 1			Patient 2			Patient 3		
Nerve	**MCV, m/s**	**DL, ms**	**CMAP, mV**	**MCV, m/s**	**DL, ms**	**CMAP, mV**	**MCV, m/s**	**DL, ms**	**CMAP, mV**
Median									
E-W	67		11.2	57		11.6	64		21.8
W-APB		2.6	11.2		4.6[a]	12.7		2.6	22.0
Ulnar									
E-W	61		4.1	60		5.5	65		10.4
W-FI		2.5	4.3		2.2	4.9		2.1	10.6
Peroneal									
K-A	51		4.7	48		3.8	51		10.1
A-EDB		5.3	4.9		3.1	4.0		3.5	11.6
	SCV, m/s		**SNAP, μV**	**SCV, m/s**		**SNAP, μV**	**SCV, m/s**		**SNAP, μV**
Median									
IIIF-W	54		30	38[a]		13	NE		NE
Ulnar									
VF-W	54		12	54		9	NE		NE
Sural									
A-sural	48		26	43		28	56		34

Abbreviations: A = ankle; APB = abductor pollicis brevis; CMAP = compound muscle action potential; DL = distal latency; E = elbow; EDB = extensor digitorum brevis; FI = first interossei; G = gastrocnemius; IIIF = third finger; K = knee; MCV = motor conduction velocity; PF = popliteal fossa; SCV = sensory conduction velocity; SNAP = sensory nerve action potential; VF = fifth finger; W = wrist.
[a] Abnormal value.

sis by direct sequencing. In brief, 50 ng of genomic DNA from the patients was amplified using the hot-start PCR method. Using a presequencing kit (USB Corp., Cleveland, OH), PCR products were purified and sequenced by dye terminator chemistry using an ABI Prism 377 DNA Sequencer (Applied Biosystems, Foster City, CA). The resulting sequences were then aligned, and mutations were evaluated using Sequencher version 4.8 sequence alignment software (Gene Codes, Ann Arbor, MI).

RESULTS **Electrophysiologic study.** Needle EMG revealed a neurogenic pattern, with a high frequency of large motor unit potentials recorded from the lower limbs of all 3 patients tested. Patient 1 showed normal sensory nerve conduction velocities (SCVs) and sensory nerve action potential of the median, ulnar, and sural nerves. Furthermore, he showed normal motor nerve conduction velocities and amplitudes of the compound muscle action potentials of the median, ulnar, and peroneal nerves. Patient 2 showed normal SCV, with a slight increase in distal latency in the median nerve and a mild decrease in SCV, suggestive of bilateral carpal tunnel syndrome. Patient 3 showed results similar to those of patient 1 (table). These findings indicate a chronic neurogenic pattern, suggesting that this family had inherited motor neuropathy.

MRI study. An axial T1-weighted MRI showed accentuated fatty infiltration of the gastrocnemius and vastus lateralis muscles (figure 2, C and D).

Resequencing analysis and control study. We identified one missense mutation, c.2677G>A (designated p.D893N), in exon 19 of *AARS*. All 4 family members considered to be clinically affected proved to have the heterozygous AARS p.D893N mutation, whereas none of the 4 unaffected relatives harbored this mutation (figure 2G). In addition, the mutation was not found in 220 East Asian (120 Chinese and 100 Japanese) control chromosomes or the chromosomes of patients with 850 inherited neuropathy nor did we find the D893N mutation in the 1000 Genomes Web site, which catalogs human genetic variations using 1,197 samples including 300 East Asian (200 Chinese) samples (http://browser.1000genomes.org).

DISCUSSION We report that an *AARS* mutation caused dHMN. A detailed investigation of the history of a family revealed 9 members over 3 generations, 4 of whom were affected individuals, consistent with a pattern of autosomal dominant transmission (figure 1). Clinical examination revealed benign wasting and weakness of the lower limbs. The diagnosis of dHMN was based on the history of autosomal dominant inheritance and electrophysiologic studies.

AARSs are a ubiquitously expressed, essential family of enzymes responsible for attaching amino acids to their cognate tRNAs in all cells and tissues. Mutations in 4 genes, *GARS*, *YARS*, *AARS*, and *KARS*, that encode AARSs have been implicated in CMT/dHMN.[5,8–10] Mutations in *GARS*, *YARS*, and *AARS* cause autosomal dominant CMT/dHMN. Two *KARS* mutations were detected in the compound heterozygous state in a patient with autosomal recessive CMT, developmental delay, self-abusive behavior, dysmorphic features, and vestibular schwannoma.[10] To elucidate the reason that mutations in ubiquitously expressed AARSs result in peripheral neuropathy, the effects of GARS, YARS, AARS, and KARS mutations in CMT/dHMN were investigated. A common pathologic mechanism for genetic disorders is a loss of gene function through altered mRNA or protein levels, although this is unusual for neurodegenerative diseases inherited in an autosomal dominant manner. Studies on G240R GARS heterozygous mutated lymphoblastoid cells did not reveal severely altered transcription, translation, or protein stability.[12] Pathogenic mechanisms such as defective aminoacylation, abnormal distribution in axons, or a combination of both are postulated to underlie CMT/dHMN, based on functional and protein localization studies of heterozygous GARS and AARS mutants.[9,12] Functional analyses of compound heterozygous mutations in *KARS* revealed severely affected enzyme activity.[10]

AARS catalyzes the attachment of alanine to its cognate tRNAs during protein synthesis. Investigation of the structure of AARS by X-ray crystallography revealed that it contains, from the N to the C terminus, an aminoacylation domain, a middle helical domain, an editing domain, and a so-called C-Ala domain.[13] The reported variant (R329H) is located in the middle helical domain, which together with the aminoacylation domain, is responsible for the complete and specific aminoacylation of AARS. The D893N variation is located in the C-Ala domain, which facilitates efficient editing by bringing together the aminoacylation and editing domains. A sequence homology search was performed to align protein sequences from multiple species, using a constraint-based multiple alignment tool (COBALT) (http://www.ncbi.nlm.nih.gov/tools/cobalt/). Aspartic acid 893 was conserved among all species analyzed (figure 2H). Thus, the D893N mutation identified in the Chinese dominant dHMN family is located in a remarkably well-conserved sequence of amino acids, suggesting that it may have a potential functional impact on AARS. Furthermore, we were able to computationally predict the effect of the D893N mutation on protein function using the MuPro (http://www.ics.uci.edu/~baldig/mutation.html) and PolyPhen-2 (http://genetics.bwh.harvard.edu/pph2/) algorithms, which gave scores of −0.334 and 0.802, respectively. MUPro scores of less than 0 indicate a decrease in protein stability, and PolyPhen-2 scores of approximately 1 indicate a prediction of pathogenicity. The D893N mutation is probably a pathogenic mutation, based on the degree of conservation of the affected residues.

Five genes (*HSPB8, HSPB1, GARS, TRPV4*, and *BCSL2*) have been described in both dHMN and CMT.[2–7] We add *AARS* on the basis of the present report. GARS and AARS are involved in common processes during protein synthesis, and the mutations reported to date were all missense mutations. Pathogenic missense mutations for autosomal dominant disease usually have a gain-of-function or dominant-negative effect. These pathogenic mutations of tRNA synthetases may directly disrupt protein synthesis.

Our data confirm that a mutation in the *AARS* gene (designated p.D893N) is associated with dominant dHMN in a Chinese family. This observation adds to a growing body of evidence that implicates specific genes/proteins in peripheral nerve function and delineates the pathologic consequences of their dysfunction.

AUTHOR CONTRIBUTIONS

Z. Zhao and Dr. Hashiguchi contributed equally to this work. Dr. Hu and Dr. Takashima designed the research. Z. Zhao, Dr. Hashiguchi, Dr. Tokunaga, Dr. Sakiyama, and Dr. Okamoto performed genetic studies. L. Zhu, H. Shen, and Dr. Hu performed clinical research and provided patient information. Z. Zhao, Dr. Hu, and Dr. Takashima wrote the article.

ACKNOWLEDGMENT

The authors thank the families described in this report for their cooperation and A. Yoshimura of Kagoshima University for her excellent technical assistance.

DISCLOSURE

The authors report no disclosures relevant to the manuscript. **Go to Neurology.org for full disclosures.**

Received October 18, 2011. Accepted in final form January 23, 2012.

REFERENCES

1. Harding AE. Inherited neuronal atrophy and degeneration predominantly of lower motor neurons. In: PJ Dyck, PK Thomas, eds. Peripheral Neuropathy. Philadelphia: WB Saunders; 1993.
2. Drew AP, Blair IP, Nicholson GA. Molecular genetics and mechanisms of disease in distal hereditary motor neuropathies: insights directing future genetic studies. Curr Mol Med 2011;11:650–665.
3. Irobi J, Van Impe K, Seeman P, et al. Hot-spot residue in small heat-shock protein 22 causes distal motor neuropathy. Nat Genet 2004;36:597–601.
4. Houlden H, Laura M, Wavrant-De Vrièze F, et al. Mutations in the HSP27 (HSPB1) gene cause dominant, reces-

sive, and sporadic distal HMN/CMT type 2. Neurology 2008;71:1660–1668.
5. Antonellis A, Ellsworth RE, Sambuughin N, et al. Glycyl tRNA synthetase mutations in Charcot-Marie-Tooth disease type 2D and distal spinal muscular atrophy type V. Am J Hum Genet 2003;72:1293–1299.
6. Windpassinger C, Auer-Grumbach M, Irobi J, et al. Heterozygous missense mutations in BSCL2 are associated with distal hereditary motor neuropathy and Silver syndrome. Nat Genet 2004;36:271–276.
7. Sambuughin N, Sivakumar K, Selenge B, et al. Autosomal dominant distal spinal muscular atrophy type V (dSMA-V) and Charcot-Marie-Tooth disease type 2D (CMT2D) segregate within a single large kindred and map to a refined region on chromosome 7p15. J Neurol Sci 1998;161:23–28.
8. Jordanova A, Irobi J, Thomas FP, et al. Disrupted function and axonal distribution of mutant tyrosyl-tRNA synthetase in dominant intermediate Charcot-Marie-Tooth neuropathy. Nat Genet 2006;38:197–202.
9. Latour P, Thauvin-Robinet C, Baudelet-Méry C, et al. A major determinant for binding and aminoacylation of $tRNA^{Ala}$ in cytoplasmic alanyl-tRNA synthetase is mutated in dominant axonal Charcot- Marie-Tooth disease. Am J Hum Genet 2010;86: 77–82.
10. McLaughlin HM, Sakaguchi R, Liu C, et al. Compound heterozygosity for loss-of-function lysyl-tRNA synthetase mutations in a patient with peripheral neuropathy. Am J Hum Genet 2010;87:560–566.
11. Cutler DJ, Zwick ME, Carrasquillo MM, et al. High-throughput variation detection and genotyping using microarrays. Genome Res 2001;11:1913–1925.
12. Antonellis A, Lee-Lin SQ, Wasterlain A, et al. Functional analyses of glycyl-tRNA synthetase mutations suggest a key role for tRNA-charging enzymes in peripheral axons. J Neurosci 2006;26:10397–10406.
13. Swairjo MA, Otero FJ, Yang XL, et al. Alanyl-tRNA synthetase crystal structure and design for acceptor-stem recognition. Mol Cell 2004;13:829–841.